A Saccharide-Based Model System for Studying the Photophysical Behavior and Singlet Oxygen Generation of Indocyanine Green

Barbara Smolak[1,ABDEF], *Klaudia Dynarowicz*[2,BCDFG], *Dorota Bartusik-Aebisher*[2,ABCDH], *Adrian Truszkiewicz*[3,BCFG], *David Aebisher*[3,ABCFH]*, *Aleksandra Kawczyk-Krupka*[4,BCFH], *Wiesław Guz*[1,ABCDEFGH]*

[1] University of Rzeszów, Medical College, Department of Diagnostic Imaging and Nuclear Medicine, ul. Warzywna 1A, 35-310 Rzeszów, Poland
[2] University of Rzeszów, Medical College, Department of Biochemistry and General Chemistry, ul. Warzywna 1A, 35-310 Rzeszów, Poland
[3] University of Rzeszów, Medical College, Department of Photomedicine and Physical Chemistry, ul. Warzywna 1A, 35-310 Rzeszów, Poland
[4] Medical University of Silesia in Katowice, Faculty of Medical Sciences in Zabrze, Department of Internal Medicine, Angiology and Physical Medicine, Center for Laser Diagnostics and Therapy, ul. Jordana 19, 40-055 Katowice, Poland

Funding: This research received no external funding.
Institutional Review Board Statement: Not applicable.
Informed Consent Statement: Not applicable.

Abstract

Introduction: Indocyanine green (ICG) is a clinically approved near-infrared fluorescent dye used in medical diagnostics, including vascular imaging, tissue perfusion assessment, and fluorescence-guided surgical procedures, and it has also been explored as a photosensitizer in photochemical applications, where its activity is associated with photoinduced energy transfer processes that can lead to the formation of reactive oxygen species, including singlet oxygen. The photophysical properties of ICG are strongly dependent on the microenvironment, and in aqueous systems the dye readily undergoes aggregation and photophysical degradation. Immobilization of ICG in saccharide-based matrices represents a potential strategy to stabilize its optical response and preserve its photosensitizing activity. The aim of this study was to investigate the absorption, fluorescence, and singlet oxygen generation of ICG immobilized in thin-film saccharide-based structures under surface-confined conditions.

Methods: Thin-film samples were prepared by incorporating ICG into a simple saccharide-based matrix based on sucrose and corn syrup. Absorption and steady-state fluorescence spectra were recorded using UV–VIS and fluorescence spectroscopy, while singlet oxygen generation was evaluated by direct detection of its characteristic near-infrared phosphorescence using time-correlated single-photon counting (TCSPC). Measurements were performed on six independently prepared samples with repeated acquisitions to ensure high reproducibility.

Results: The ICG–saccharide-based films exhibited a stable absorption maximum at approximately 790 nm and a fluorescence maximum at 830 nm, with highly consistent spectral profiles across all samples. Importantly, a distinct singlet oxygen phosphorescence band in the 1260–1270 nm range was consistently observed, providing direct experimental evidence that immobilization of ICG within thin saccharide-based films does not suppress its ability to generate singlet oxygen. The observed spectral features indicate effective stabilization of the dye and reduced aggregation-related quenching.

Conclusions: Thin-film saccharide-based matrices provide a simple and reproducible environment in which the characteristic optical and photochemical properties of indocyanine green can be preserved under surface-confined conditions. The presented system should be regarded as a surface-confined model for photochemical investigations of immobilized

Medicine Physicist & Engineer 1/2026 vol. 1
received: 14.04.2026; corrected: 29.04.2026; accepted: 08.05.2026

Author Contributions:
A – Conceptualization, B – Validation, C – Formal analysis, D – Resources, E – Writing—original draft preparation, F – Writing—review and editing, G – Visualization, H – Supervision.
All authors have read and agreed to the published version of the manuscript.

photosensitizers rather than a direct surrogate of *in vivo* conditions, where protein binding and biological selectivity govern ICG behavior.

Keywords: Indocyanine green; fluorescence; absorption; saccharide-based matrix; singlet oxygen; photochemistry; photodynamic therapy

Introduction

Fluorescence is a process involving the absorption of a photon by a molecule followed by the emission of light of lower energy, resulting in a characteristic Stokes shift. Owing to their high sensitivity and the possibility of selective detection, fluorescence methods constitute a key tool in chemical analysis, molecular biology, and medical diagnostics. The emission properties of fluorophores are strongly dependent on their environment, which means that changes in the surrounding matrix can significantly affect the character and intensity of the spectra [1-3].

One of the most commonly used fluorescent dyes is indocyanine green, which exhibits intense absorption and emission in the near-infrared region [4]. This dye has been used for many years in medical imaging, and its ability to generate reactive oxygen species also makes it suitable as a photosensitizer in photodynamic therapy (PDT) [5,6]. In the excited state, ICG can undergo intersystem crossing to the triplet state and subsequently transfer energy to molecular oxygen, leading to the formation of singlet oxygen ($^1O_2$), which is crucial for the destruction of pathological tissues [6,7]. A major limitation of ICG, however, is its susceptibility to photodegradation and its tendency to aggregate, which reduces fluorescence intensity and the efficiency of $^1O_2$ generation [8].

Indocyanine green is a hydrophilic dye that is readily soluble in water but can also dissolve in certain organic solvents. It exhibits strong light absorption at approximately 780 nm and emission in the 800–850 nm range, enabling its use in fluorescence imaging and other near-infrared optical diagnostic techniques. ICG shows a tendency to aggregate in aqueous solutions, which may affect its optical properties. It belongs to the class of cyanine dyes, which are widely used in optics and spectroscopy due to their unique absorption and fluorescence characteristics [9].

Indocyanine green has long been applied in medical diagnostics as a fluorescent dye. Thanks to its unique optical properties, it enables high-precision imaging of biological structures, while its near-infrared emission allows high-contrast visualization. After administration into the body, ICG binds to plasma proteins, which determines its specific pharmacokinetic properties: following intravascular injection, it is distributed with the bloodstream, subsequently taken up by the liver, and excreted into the bile. In addition, the photosensitizing properties of the dye allow its use in procedures based on the generation of reactive oxygen species, which is exploited in modern diagnostic and therapeutic techniques [10].

In oncological diagnostics, ICG is used for fluorescence visualization of lymphatic drainage and sentinel lymph nodes as an alternative or complement to conventional sentinel lymph node biopsy procedures. Reports indicate high diagnostic effectiveness, good visualization, and a favorable safety profile of ICG; however, a limitation remains the lack of selective labeling of cancer cells, which hinders direct assessment of metastases [11]. In liver surgery, ICG is applied for fluorescence visualization of bile ducts and selected hepatic lesions; the dye absorbs light in the near-infrared range and emits fluorescence at around 830 nm, enabling intraoperative detection of certain lesions, although the effectiveness of this technique decreases for deeper-located foci [12].

ICG is also used in the diagnosis of lymphatic drainage disorders. Fluorescence lymphography with ICG enables real-time imaging of superficial lymph flow and may exhibit high sensitivity in detecting abnormalities of lymphatic vessels, particularly when combined with methods assessing changes in subcutaneous tissues [13]. In recent years, attention has also been drawn to the use of ICG fluorescence for intraoperative identification of parathyroid glands, which may improve surgical precision and limit the extent of procedures, although this method still requires further clinical studies and access to specialized imaging equipment [14]. Furthermore, ICG fluorescence imaging is used to assess tissue microperfusion in real time across various surgical disciplines, potentially supporting intraoperative decision-making and monitoring the effectiveness of revascularization procedures [15].

Indocyanine green can also act as a photosensitizer in photodynamic therapy, because after absorption of light (780–810 nm) it transitions to an excited state and subsequently—via intersystem crossing—to the triplet state, enabling energy transfer to molecular oxygen and the generation of ($^1O_2$). Singlet oxygen initiates processes leading to damage of cellular structures (including lipids, proteins, and DNA), ultimately resulting in the death of target cells [16]. Compared with classical photosensitizers (e.g., porphyrins or phthalocyanines), ICG is characterized by a lower quantum yield of $^1O_2$ generation, which results, among other factors, from its susceptibility to photodegradation and limited efficiency of intersystem crossing. The literature indicates that improvements in efficiency may be achieved by increasing the stability and bioavailability of the dye, for example through conjugation with proteins or nanoparticles [17,18].

Photodynamic therapy is a treatment modality that employs a photosensitizer, light of an appropriate wavelength, and oxygen present in tissues. Upon excitation of the photosensitizer, photochemical reactions are initiated that lead to the generation of reactive oxygen species, including singlet oxygen, which cause damage to cellular structures and death of target cells

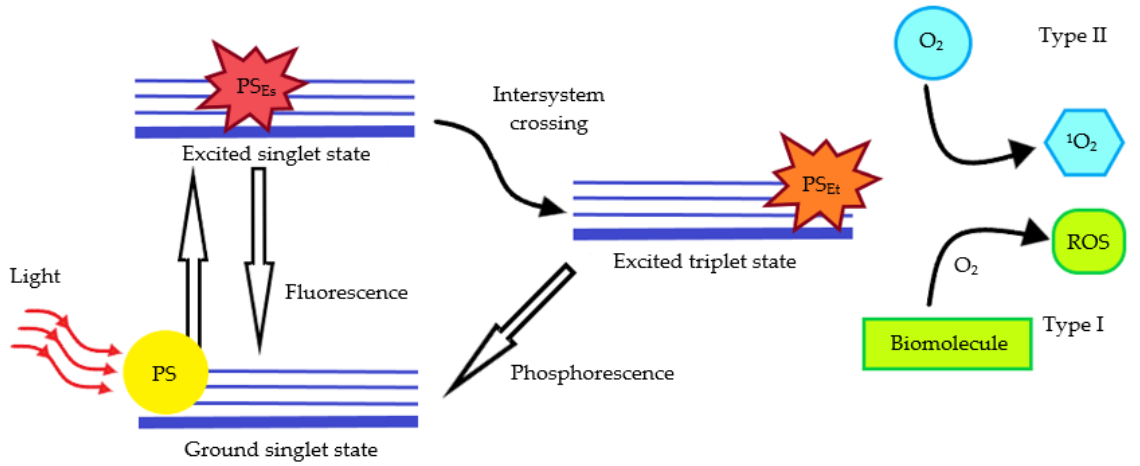

Fig. 1 *Schematic illustration of the photophysical and photochemical pathways relevant to photodynamic action: excitation of the photosensitizer (PS) to the singlet excited state (PS*), intersystem crossing to the triplet state ($^3PS^*$), and subsequent type I and type II photochemical pathways involving molecular oxygen, leading to the formation of reactive oxygen species (ROS) and singlet oxygen ($^1O_2$). In this study, singlet oxygen formation was evaluated by direct detection of its characteristic phosphorescence in the 1260–1270 nm range. PS, photosensitizer; PS*, excited singlet state; $^3PS^*$, excited triplet state; O_2, molecular oxygen; $^1O_2$, singlet oxygen; ROS, reactive oxygen species. Source: Own elaboration.*

[19]. Advances in nanotechnology and materials engineering promote improved selectivity and bioavailability of photosensitizers, thereby increasing the effectiveness of PDT while limiting toxicity to healthy tissues [20]. The PDT mechanism (Fig. 1) involves excitation of the photosensitizer to the singlet state, transition to the triplet state, and type I and type II reactions leading to the generation of ROS and/or $^1O_2$, which form the basis of the therapeutic effect [21-23].

Porphyrin- and phthalocyanine-based photosensitizers have demonstrated strong photodynamic efficacy in both oncological and antimicrobial applications; however, their clinical use may in some cases be limited by absorption predominantly in the visible spectral range, shallow tissue penetration, prolonged skin photosensitivity, and complex pharmacokinetics [24-26].

In contrast, cyanine dyes represent an alternative class of photosensitizers that operate in the near-infrared (NIR) optical window, where light penetration in biological tissues is significantly enhanced. Among them, indocyanine green (ICG) is of particular interest due to its long-standing clinical approval, favorable safety profile, and well-established use in fluorescence-guided diagnostics [27-28]. In addition to its imaging capabilities, ICG can act as a photosensitizer by undergoing intersystem crossing and transferring energy to molecular oxygen, resulting in singlet oxygen generation, which enables its application in photodynamic therapy [27-29].

Although the intrinsic singlet oxygen quantum yield of ICG is generally lower than that of porphyrin- or phthalocyanine-based photosensitizers, its unique combination of near-infrared absorption, rapid systemic clearance, and theranostic potential distinguishing it from many porphyrin- and phthalocyanine-based PDT photosensitizers [27,28]. Importantly, numerous studies indicate that the photophysical limitations of ICG—such as aggregation, photodegradation, and reduced intersystem crossing efficiency—can be mitigated through appropriate stabilization strategies, including incorporation into polymeric, nanoparticulate, or biopolymeric matrices [28,29]. These approaches not only improve the stability of ICG but also support its continued ability to generate singlet oxygen, thereby justifying further investigation of immobilized ICG systems. A concise comparison of representative photosensitizer classes commonly used in photodynamic therapy is provided in Table 1 to place indocyanine green in the broader context of established PDT agents and to clarify the rationale for its selection in this study, particularly with respect to near-infrared absorption, tissue penetration, and suitability for surface immobilization.

In the context of PDT, an important advantage of ICG is the possibility of simultaneously monitoring its distribution via near-infrared fluorescence, which supports real-time guidance in photoactivated procedures. Research on the application of ICG in photodynamic and photothermal concepts also

Table 1 *Comparison of selected photosensitizer classes used in photodynamic therapy*

Photosensitizer class	Main absorption range	Singlet oxygen generation	Tissue penetration	Clinical status	Key limitations
Porphyrins	Visible (400–650 nm)	High	Low–moderate	Clinical / preclinical	Skin photosensitivity, slow clearance
Chlorins	Visible–red (600–700 nm)	High	Moderate	Preclinical / clinical	Limited NIR absorption
Phthalocyanines	Red (650–700 nm)	High	Moderate	Preclinical	Poor solubility, aggregation
Cyanine dyes (ICG)	Near-infrared (750–810 nm)	Moderate	High	Clinically approved	Aggregation, photodegradation

Source: Own elaboration.

includes strategies aimed at improving its stability, for example through association with carriers such as liposomes, polymers, or nanoparticles, with the goal of enhancing performance and controlling local availability [30-32].

Indocyanine green is a near-infrared cyanine dye whose photophysical behavior strongly depends on its molecular environment. Its extended conjugated polymethine system and amphiphilic character promote aggregation and photodegradation in aqueous media, which can significantly limit photodynamic efficiency. These properties have motivated the development of stabilization strategies based on immobilization in polymeric and biopolymeric matrices.

In order to reduce photodegradation and aggregation of indocyanine green, its stabilization on various surfaces and within polymer matrices has been investigated. These systems create a hydrophilic microenvironment that favors the preservation of the photophysical properties of the dye. It has been shown that immobilization of ICG in thermosensitive hydrogels allows retention of its characteristic near-infrared absorption and fluorescence, as well as effective utilization of its photothermal and photodynamic properties in postoperative therapies and tissue markers [33,34]. Similar effects have been achieved in composite polymer and silk fibers, where incorporation of ICG into fibrillar structures resulted in a stable fluorescence signal and controlled photothermal interactions [35,36]. Functional stabilization of ICG has also been observed in natural protein matrices, such as gelatin, in which the dye retained its ability to absorb NIR radiation and convert light energy into heat, finding application in photothermal therapies and tumor microenvironment–responsive systems [37]. Moreover, hybrid hydrogels based on yeast cell wall components have demonstrated that appropriately designed biopolymer matrices can effectively protect ICG and enable its use in combination therapies that integrate photothermal effects with immunological responses [38]. These examples confirm that soft, biocompatible polymeric and biopolymeric surfaces constitute effective environments for stabilizing ICG while preserving its key optical and photochemical properties.

Among the matrices reported in the literature for stabilizing indocyanine green, particular attention has been paid to polysaccharides, which are natural biopolymers with diverse structures and physicochemical properties. Their use as immobilizing matrices allows improvement of the stability and photophysical properties of ICG. Polysaccharides are natural biopolymers composed of monosaccharide units linked by glycosidic bonds. They may occur in linear or branched forms, and their structure—depending on the type of bonds, degree of branching, and presence of functional groups—confers a wide range of physicochemical properties [39]. Important representatives include homopolysaccharides such as cellulose, starch, and glycogen, as well as heteropolysaccharides such as heparin and hyaluronic acid.

In living organisms, polysaccharides fulfill structural, storage, and regulatory functions, and their macromolecular nature enables the formation of three-dimensional networks that stabilize bioactive molecules [40,41]. In the context of photochemistry, they play a particularly important role as matrices that restrict fluorophore mobility, prevent aggregation, and modify microenvironmental properties such as polarity, viscosity, and oxygen availability [42,43]. All of these factors influence fluorescence intensity, intersystem crossing efficiency, and the effectiveness of singlet oxygen generation [44,45]. Moreover, owing to their biocompatibility and non-toxicity, polysaccharides constitute an attractive platform for biomedical applications, including the design of therapeutic materials and drug delivery systems [42,46].

Thin-film saccharide-based surfaces were selected as model matrices due to their favorable physicochemical properties and relevance to biomedical applications. Compared with bulk hydrogels or solution-based systems, thin films provide uniform light penetration, efficient oxygen diffusion, and direct optical access to immobilized photosensitizers, which are critical factors for photodynamic processes dependent on light–matter interactions and singlet oxygen generation [47]. Surface-confined systems also enable improved control over dye aggregation, spatial distribution, and photostability in comparison with dispersed carriers.

Importantly, the aim of the present study is not to reproduce biological environments or to optimize clinical photodynamic therapy performance, but to establish a simplified surface-confined photophysical model enabling controlled investigation of dye–matrix interactions and singlet oxygen generation under well-defined non-biological conditions.

Polysaccharides are particularly attractive materials for the fabrication of such thin-film structures owing to their natural origin, biocompatibility, non-toxicity, and ability to form hydrogen-bonded networks that stabilize photoactive compounds. Numerous studies have demonstrated that polysaccharide-based hydrogels and films can effectively host photosensitizers, including porphyrins and related compounds, while preserving their photophysical activity and enabling controlled photodynamic action [48,49].

Importantly, the present work employs a simplified low-molecular-weight saccharide-based system rather than true high-molecular-weight polysaccharides. These materials nevertheless provide a useful conceptual framework for understanding matrix-induced stabilization effects. Moreover, carbohydrate-based matrices reported in the literature are highly relevant for medical and photodynamic applications, as they can be integrated into surface-based platforms such as coatings, wound dressings, and light-activated therapeutic materials [49–51].

In this context, thin-film saccharide-based matrices constitute a simplified yet application-oriented model system for investigating the photophysical behavior and singlet oxygen generation of immobilized photosensitizers under surface-confined conditions.

Despite the growing interest in ICG systems embedded in biopolymers, detailed studies describing the influence of simple saccharide-based matrices- such as sucrose mixtures, sugar syrups, or colloidal structures - on the spectral and photochemical properties of ICG are still lacking. Understanding these relationships is crucial both from the perspective of fundamental photophysics and potential practical applications.

The aim of the present study was not to reproduce biological environments or to evaluate clinical photodynamic therapy performance, but rather to investigate the photophysical behavior of immobilized indocyanine green in a simplified surface-confined model system. In addition, the ability to generate singlet oxygen in ICG–saccharide-based systems was investigated, and the extent to which matrix microstructure affects the efficiency of this process was evaluated. The results provide new insights into dye–biopolymer interactions and may contribute to the design of stable and functional materials for optical imaging and photodynamic therapy.

The proposed saccharide-based model system enables investigation of indocyanine green photophysics and singlet oxygen generation under surface-confined conditions, providing insight into dye behavior at solid–liquid interfaces that cannot be obtained from bulk solution studies.

Materials and Methods

The samples were prepared using 59.1 mg of sucrose (Merck, Darmstadt, Germany), 44.36 mL of deionized water, 27.5 mL of white corn syrup obtained from corn starch (Corn Syrup®, Korea), and 3 mg of the dye indocyanine green (ROTH®, Germany). Standard laboratory equipment was used for solution preparation, including a 250 mL glass beaker, a glass stirring rod, a magnetic stir bar (1 cm × 0.5 cm) with an AREC.X heating magnetic stirrer (Velp Scientifica), as well as a laboratory spatula, weighing boat, analytical balance, pipette, microscope slide, and a quartz cuvette intended for spectrophotometric measurements.

Sugars and solvents (sucrose, water, and corn syrup) were transferred to a 250 mL beaker to obtain a final volume of 132.9 mL. The mixture was homogenized using a magnetic stirrer for 10 min. Subsequently, 3 mg of indocyanine green was weighed on an analytical balance and gradually added to the mixture under continuous stirring until a uniform coloration was obtained. To evaluate the influence of dye concentration on the spectral response, additional mixtures containing 2 mg and 1 mg of ICG were initially prepared. These lower concentrations produced significantly weaker fluorescence and singlet oxygen signals under the applied experimental conditions, which limited reliable detection using the available instrumentation. Therefore, the detailed spectroscopic analysis presented in this work was performed using samples containing 3 mg of ICG, which provided an adequate signal-to-noise ratio. It should be noted that this concentration was selected primarily for experimental detectability rather than to reproduce clinically used ICG concentrations. A small amount of the solution was placed on a microscope slide and left to thicken for one week under aluminum foil protection. Additional portions of the liquid sample were transferred to a quartz cuvette for absorption and fluorescence analysis.

Thickness evaluation and optical inspection of the prepared saccharide-based film were performed using an Olympus BX51 fluorescence microscope. The approximate average thickness of the formed saccharide-based coating was about 0.5 mm, as determined from calibrated optical measurements. The BX51 is a research-grade upright optical microscope designed for bright-field, fluorescence, and transmitted-light imaging, equipped with high numerical aperture objectives and modular fluorescence illumination. The system enables precise visualization of sample morphology and dimensional assessment through calibrated optical imaging. Microscopic observations were carried out under transmitted-light conditions. The film formed directly on the microscope slide was additionally used for qualitative assessment of surface morphology and thickness estimation, allowing evaluation of the geometric characteristics of the investigated model system [52].

Absorbance spectra were recorded using an Agilent Cary 60 UV–VIS spectrophotometer. This is an advanced analytical instrument designed for measuring radiation absorption in the ultraviolet and visible ranges, covering wavelengths from 190 to 1100 nm. The instrument employs a long-life xenon lamp as the light source, providing high signal stability and good measurement reproducibility. The spectral resolution of the device is 1.5 nm, enabling precise identification of absorption bands of the investigated compounds. The operating principle of the spectrophotometer is based on the Beer–Lambert law, according to which absorbance is proportional to the concentration of the substance and the optical path length [53,54]. To improve signal stability, the thickened material deposited on a microscope slide was placed close to the light source inside the measurement chamber.

Fluorescence emission spectra were obtained using an Agilent Cary Eclipse fluorescence spectrometer. This instrument enables fluorescence measurements over excitation and emission wavelength ranges from 200 to 900 nm, with a spectral resolution of 1.5 nm. A xenon lamp serves as the excitation light source, characterized by high stability and emission intensity. The Cary Eclipse allows rapid wavelength switching (below 0.1 s), enabling dynamic spectral scanning and analysis of photophysical processes. Fluorescence measurements involve recording the intensity of light emitted by the sample after excitation, with emission intensity being proportional to the fluorophore concentration in the sample [55]. Due to geometric limitations of the solid-sample holder, liquid aliquots of the mixture were analyzed in a quartz cuvette.

Time-resolved fluorescence measurements and analyses of singlet oxygen generation were performed using a FluoTime 300 spectrometer operating in the time-correlated single-photon counting (TCSPC) mode. This system is a fully automated,

high-sensitivity fluorescence spectrometer that enables recording of fluorescence and phosphorescence lifetimes with temporal resolution reaching the picosecond range. The instrument is equipped with advanced measurement optics, Czerny–Turner monochromators, and highly sensitive photomultiplier detectors, allowing precise analysis of emission over a wide spectral range. The detection system enables registration of very low-intensity signals, including the characteristic phosphorescence of singlet oxygen in the region of approximately 1270 nm [56-58].

The generation of singlet oxygen by ICG was evaluated using 9,10-anthracenediyl-bis(methylene)dimalonic acid (ABDA) as a chemical probe. ABDA reacts selectively with singlet oxygen, leading to a progressive decrease in its absorbance at 380 nm, which was monitored during irradiation. Since indocyanine green is known to undergo photooxidative degradation upon interaction with singlet oxygen, effectively acting as a self-sensitized trap, the decrease in ABDA absorbance was used as an indirect measure of singlet oxygen production.

Measurements were performed for ICG dissolved in water and compared with a reference photosensitizer, methylene blue (MB), characterized by a known singlet oxygen quantum yield:

$$\Phi_{\Delta std\ (MB)} = 0.52.$$

Under conditions where the concentration of ABDA is significantly lower than that of dissolved oxygen and irradiation intensity remains constant, the reaction can be treated as pseudo-first-order with respect to ABDA concentration. In this approach, A_0 represents the initial absorbance of ABDA at 380 nm prior to irradiation, while A_t denotes the absorbance measured after irradiation time t. Because absorbance is directly proportional to ABDA concentration according to the Beer–Lambert law, the decrease in absorbance can be described using the integrated first-order rate Equation (1):

$$\ln\left(\frac{A_0}{A_t}\right) = k \cdot t, \quad (1)$$

Linear regression analysis of $\ln\left(\frac{A_0}{A_t}\right)$ versus irradiation time provided the rate constants:

$$k_{std\ (MB)} = 0.00467\ s^{-1}$$

$$k_{ICG} = 0.00015\ s^{-1}.$$

The singlet oxygen quantum yield (Φ_Δ) of ICG was determined using a relative method based on comparison with the reference photosensitizer. The quantum yield was calculated according to Equation (2):

$$\Phi_{\Delta(ICG)} = \Phi_{\Delta std} \cdot (k_{ICG} / k_{std}), \quad (2)$$

where $\Phi_{\Delta std}$ is the singlet oxygen quantum yield of methylene blue, and k_{ICG} and k_{std} correspond to the pseudo-first-order rate constants obtained under identical experimental conditions for ICG and MB, respectively.

Assuming identical absorbance at the excitation wavelength for both photosensitizers ($A_{ex} \approx 0.1$), the light absorption correction factor cancels out, allowing direct comparison of the rate constants.

Substituting the experimentally obtained values into Equation (2) gives:

$$\Phi_{\Delta(ICG)} = 0.52 \times \left(\frac{0.00015}{0.00467}\right) \quad (3)$$

which yields:

$$\Phi_{\Delta(ICG)} = 0.0167 \quad (4)$$

Thus, the singlet oxygen quantum yield of ICG in aqueous solution was estimated as:

$$\Phi_\Delta \approx 0.017\ (\approx 1.6\%).$$

It should be emphasized that the above quantum yield value represents the intrinsic singlet oxygen generation efficiency of ICG in aqueous solution under standard reference conditions. The ABDA assay was not intended to quantify singlet oxygen production within the saccharide-based thin-film matrix, but rather to provide a comparative photochemical baseline independent of matrix effects. Evaluation of singlet oxygen formation in the surface-confined saccharide-based system was performed separately by direct detection of its characteristic phosphorescence at approximately 1270 nm using TCSPC measurements.

All measurements were performed for six independently prepared samples, each of which was analyzed multiple times. The obtained spectra exhibited high reproducibility, confirming the stability of the applied sample preparation procedure and the reliability of the measurement methods used.

Results

To ensure the reliability and reproducibility of the results, measurements were performed for six independently prepared samples. Each sample was subjected to multiple measurement analyses, which demonstrated high consistency of the obtained data. The recorded spectra exhibited nearly identical profiles and reproducible positions of the emission maximum, confirming the stability of the experimental system and the reliability of the applied methodology. Representative plots illustrating the characteristic results obtained during the measurements are presented below.

From the collected series of results, the plots shown as figures 2 and 3 were generated. Figure 2 presents the dependence of absorption of the saccharide-based matrix containing ICG on wavelength.

The presented graph illustrates the absorption spectrum of a solution containing indocyanine green, a fluorescent dye widely used in medicine and molecular biology. The characteristic shape of the absorption curve reflects the unique spectral properties of this compound, which are crucial for its diagnostic and therapeutic applications.

The observed absorption profile shows a distinct minimum at shorter wavelengths, followed by a gradual increase

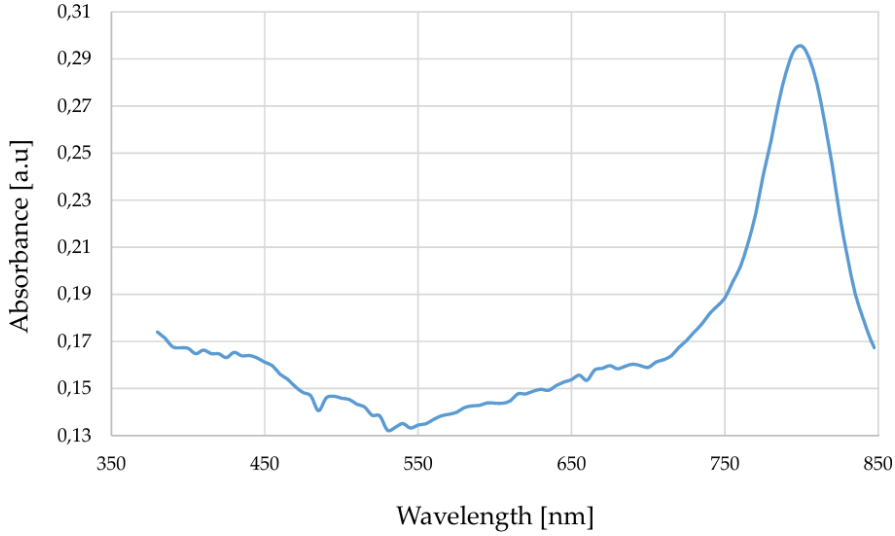

Fig. 2 *Absorbance spectrum of the saccharide-based matrix containing indocyanine green*
Source: Own elaboration.

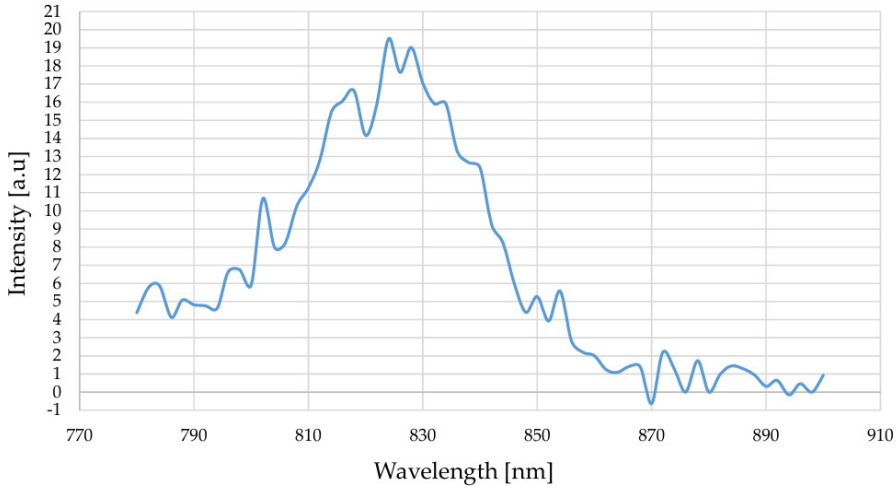

Fig. 3 *Steady-state fluorescence emission spectrum of the saccharide-based matrix containing indocyanine green*
Source: Own elaboration.

in absorption toward the near-infrared region. In this range, a pronounced absorption maximum is visible at a wavelength of approximately 790 nm. This value is slightly shifted relative to the absorption maximum of pure indocyanine green in aqueous solution, which according to the literature typically occurs at around 780 nm. Owing to its ability to absorb and emit radiation in the NIR region, ICG is used, among others, in fluorescence angiography, intraoperative monitoring of tissue perfusion, and modern cancer imaging techniques.

The ability to selectively absorb and emit light in the near-infrared range makes ICG an exceptionally useful optical contrast agent, enabling noninvasive visualization of biological structures with high precision. As a result, it plays a key role in medical imaging techniques, combining high detection sensitivity with a favorable safety profile in clinical applications. Figure 3 presents changes in fluorescence intensity as a function of wavelength for the saccharide-based matrix containing ICG.

The steady-state fluorescence emission spectrum of indocyanine green incorporated into the saccharide-based matrix is presented in Figure 3. The spectrum exhibits a pronounced emission band in the near-infrared region, with the fluorescence maximum observed at λ_{max} = 826 nm. Minor fluctuations in the spectral trace are attributed to instrumental noise and baseline correction effects at low signal intensity. This value is consistent with the characteristic near-infrared emission of indocyanine green reported in the literature and reflects the influence of the saccharide-based environment on the spectral position of the emission band.

At wavelengths above approximately 860 nm, the recorded fluorescence intensity approaches zero and slightly negative values are observed. These negative intensities do not represent physical emission but arise from background subtraction and instrumental noise near the detection limit of the spectrometer. Such behavior is commonly observed in steady-state

fluorescence measurements at low signal levels and does not affect the determination of the emission maximum.

The fluorescent properties of ICG enable its widespread use in vascular imaging, monitoring of tissue perfusion, and advanced techniques for detecting neoplastic lesions. Owing to its high sensitivity and operation in the NIR range, indocyanine green remains one of the most important fluorescent dyes used in contemporary medicine and biological sciences. Measurement of singlet oxygen phosphorescence generated by the ICG–saccharide-based sample was performed using the FluoTime 300 system (Fig. 4).

Figure 4 presents the emission spectrum of singlet oxygen generated in a sample containing indocyanine green embedded in saccharide-based matrix. The spectrum exhibits a distinct emission band with a maximum in the range of 1260–1270 nm, characteristic of singlet oxygen phosphorescence. The observed spectral profile indicates that the recorded signal originates from a single photochemical process associated with singlet oxygen generation.

The kinetics of ABDA photobleaching induced by singlet oxygen generation were analyzed by plotting $\ln(A_0/A_t)$ as a function of irradiation time, as shown in Figure 5. The obtained dependencies exhibit linear behavior for both the reference photosensitizer (methylene blue, MB) and the investigated sample containing indocyanine green (ICG), confirming pseudo-first-order reaction kinetics under the applied experimental conditions. The steeper slope observed for MB indicates a significantly higher rate of singlet oxygen generation compared to ICG, consistent with the known higher singlet oxygen quantum yield of the reference compound. In contrast, the ICG sample shows a markedly lower slope, reflecting reduced photochemical efficiency in aqueous solution. The linear fits presented in Figure 5 were used to determine the pseudo-first-order rate constants, which served as the basis for calculating the relative singlet oxygen quantum yield of ICG. The high linearity of the data confirms good reproducibility of the measurements and supports the validity of the applied kinetic model.

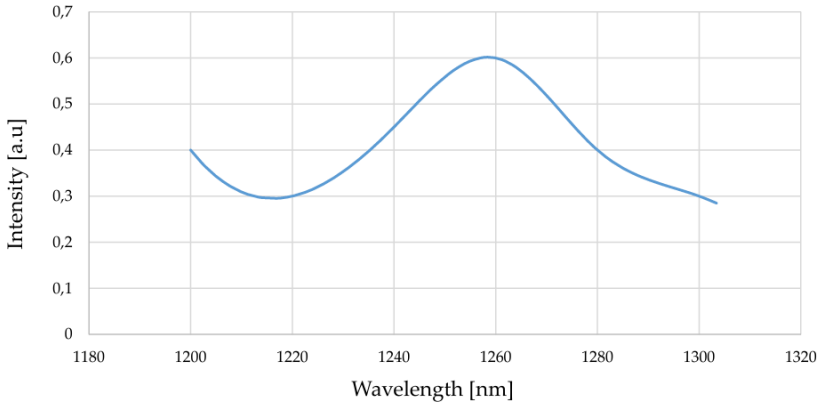

Fig. 4 *Singlet oxygen phosphorescence spectrum of the ICG-saccharide-based matrix recorded using time-correlated single-photon counting (TCSPC)*
Source: Own elaboration.

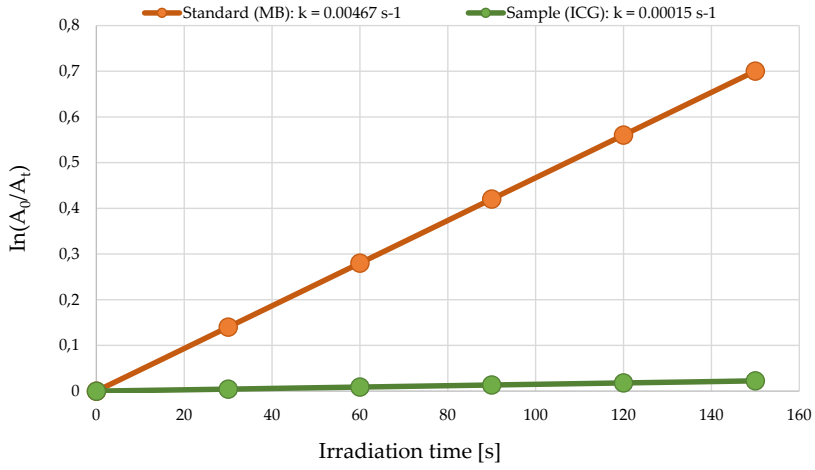

Fig. 5 *Kinetics of ABDA photobleaching. Plot of $\ln(A_0/A_t)$ vs irradiation time showing linear fits for MB (standard) and ICG (sample)*
Source: Own elaboration.

The presence of a well-defined emission maximum and the characteristic asymmetric spectral profile indicate emission originating from a single, well-identified photochemical process—namely, the generation of singlet oxygen. These results confirm the functionality and effectiveness of the ICG–saccharide-based system as a potential source of singlet oxygen for medical applications, particularly in photodynamic therapy (PDT), where selective generation of reactive oxygen species plays a key therapeutic role.

For comparison, the fluorescence maximum of ICG itself occurs at approximately 810 nm, as confirmed in the earlier spectral analysis. This demonstrates that singlet oxygen emission occurs in a completely different wavelength range, facilitating selective detection of this process using appropriate optical filters and detectors.

Discussion

The conducted studies demonstrated that indocyanine green incorporated into a saccharide-based matrix exhibits stable and reproducible spectral properties in both absorption and fluorescence ranges. The absorption maximum located at approximately 790 nm is in good agreement with literature data, according to which the typical absorption peak of ICG in aqueous solution occurs around 780 nm [4,59]. The slight spectral shift observed in our system may result from interactions between the dye and the saccharide-based matrix, which affect local polarity and the degree of molecular aggregation. Such effects have previously been reported for ICG in polymeric or micellar environments, where restricted dye mobility led to changes in the energies of electronic states [60-62].

The fluorescence spectrum with a maximum at approximately 830 nm is consistent with the characteristic near-infrared emission properties of ICG [63]. Because indocyanine green is known to exhibit concentration-dependent H- and J-aggregation as well as self-quenching phenomena, particular attention was paid to the spectral features indicative of aggregation under the investigated loading. The absorption spectrum does not exhibit a pronounced secondary band in the 700–730 nm region typically associated with strong H-aggregate formation, nor a distinct red-shifted band characteristic of J-aggregates. This suggests that, within the applied saccharide-based matrix and loading conditions, ICG is present predominantly in monomeric or weakly aggregated form. Furthermore, the high reproducibility of fluorescence intensity and spectral profile across independently prepared samples indicates that strong concentration-induced self-quenching is unlikely within the investigated range. While a systematic concentration-dependent study would provide additional quantitative insight, the present spectral characteristics support the conclusion that severe aggregation effects do not dominate under the applied experimental conditions. In clinical practice, indocyanine green is typically administered at concentrations on the order of 1.0–2.5 mg/ml depending on the diagnostic procedure. Variations in dye concentration may influence aggregation behavior, fluorescence intensity, and the efficiency of singlet oxygen formation, as reported in previous studies. A systematic investigation of concentration-dependent effects was beyond the scope of the present work and may represent an important direction for future studies aimed at relating model systems more directly to clinically relevant conditions.

The literature emphasizes that the presence of polysaccharides can stabilize the excited state and reduce dynamic quenching processes, which corresponds well with the high spectral reproducibility and low noise levels obtained in this study [64]. Rather than demonstrating active stabilization relative to other systems, the present results indicate that the saccharide-based thin film provides a controlled microenvironment enabling reproducible photophysical characterization of immobilized ICG [65]. Our results indicate that the applied thin-film saccharide-based surface provides conditions favorable for maintaining stable photophysical properties of the dye.

The sucrose–corn syrup matrix used in this study was not intended to reproduce the full biochemical complexity of biological tissues or fluids. The significance of the present system lies in its role as a reductionist photophysical model rather than a biomimetic or clinically optimized platform. By employing a simplified saccharide-based environment, the study isolates fundamental dye–matrix interactions and enables investigation of aggregation behavior, spectral stability, and singlet oxygen generation under surface-confined conditions. Such controlled model systems are widely used in photophysical research to decouple intrinsic material behavior from biological complexity, providing mechanistic insight that complements rather than replaces biological or clinical studies. The saccharide-based thin-film system employed in this study should not be interpreted as a direct surrogate of biological or clinical environments. Instead, it represents a simplified and highly controlled model designed to isolate fundamental photophysical and photochemical parameters of immobilized indocyanine green under surface-confined conditions. Such reductionist model systems are commonly used to decouple matrix-induced effects from complex biological interactions, including protein binding, enzymatic activity, and heterogeneous tissue environments. The primary goal of the present work was therefore mechanistic rather than translational, focusing on stabilization effects, aggregation behavior, and singlet oxygen generation in a defined non-biological microenvironment. Instead, it was selected as a simplified saccharide-based model system characterized by high viscosity, hydrogen-bonding capability, and restricted molecular mobility. Such properties are typical of high-molecular-weight polysaccharide-based hydrogels and thin films; although the present study employs a simplified saccharide-based matrix composed of low-molecular-weight saccharides, these systems share similar physicochemical characteristics such as hydrogen bonding and restricted molecular mobility [64].

Similar saccharide-based model matrices are commonly employed in photophysical and photochemical studies to isolate specific environmental parameters affecting dye behavior, independently of protein binding or metabolic effects, and serve as conceptual reference systems for simplified saccharide-based environments such as the model used in the present work. This approach enables systematic investigation of fundamental dye–matrix interactions under well-controlled conditions and has been widely used in studies of fluorescent dyes and photosensitizers incorporated into polymeric and biopolymeric environments [64-66]. Accordingly, the present work focuses on the intrinsic photophysical response of indocyanine green in a saccharide-rich microenvironment rather than on direct simulation of *in vivo* conditions. It is well established that in biological fluids indocyanine green rapidly binds to plasma proteins, particularly human serum albumin and lipoproteins, which leads to pronounced shifts in absorption and fluorescence spectra as well as changes in quantum yield and biodistribution [67,68]. As a consequence, the behavior of ICG observed in the present protein-free saccharide-based matrix should not be directly extrapolated to living organisms, where strong interactions with plasma proteins significantly influence its photophysical properties. Nevertheless, understanding the intrinsic photophysical properties of ICG in non-protein, viscous saccharide-rich environments constitutes an important preliminary step toward the rational design of more complex biopolymer-based systems. Such systems may include protein-containing, hybrid, or tissue-mimicking matrices intended for photomedical and photodynamic applications, where controlled stabilization of the photosensitizer and preservation of its optical and photochemical activity are essential [43,49,66].

Polysaccharides belong to a group of natural biopolymers that have gained significant importance in modern medicine, particularly in theranostics, understood as the integration of diagnostics and therapy within a single system. Due to the presence of numerous reactive functional groups, polysaccharides can be relatively easily modified by conjugation with nanoparticles, therapeutic agents, and medical imaging probes, while maintaining high biocompatibility and biodegradability [66]. Particular interest has been focused on nanostructured polysaccharide systems, including those based on chitosan and hyaluronic acid, which exhibit potential for precise drug delivery and real-time monitoring of their distribution.

In the context of nanomedicine, polysaccharides are also used as biocompatible coatings for nanoparticles, including magnetic metal oxide nanoparticles, imparting additional functionalities such as controlled interaction with the biological environment and responsiveness to environmental stimuli [69]. The application of polysaccharides in such systems has been demonstrated, among others, in cancer therapy, where they may enhance selective nanoparticle accumulation within tumors and reduce adverse effects, finding use in nanothermotherapy and molecular imaging techniques [70]. Polysaccharides have also been applied in cardiovascular diagnostics; for example, fucoidans capable of binding P-selectin have been used as imaging probes in SPECT and MRI techniques [71].

Owing to their high biocompatibility and susceptibility to chemical modification, polysaccharides also serve as carriers for contrast agents in medical imaging. A well-studied example is chitosan, which in the form of nanoparticles has been applied in magnetic resonance imaging and computed tomography, enabling precise delivery of contrast agents to selected tissues and improving diagnostic sensitivity. Importantly, modified chitosan-based systems may combine diagnostic and therapeutic functions, fitting into the concept of precision medicine [72,73].

An important experimental observation of this work was the detection of singlet oxygen emission with a distinct maximum in the 1260–1270 nm range, characteristic of $^1O_2$ phosphorescence [74]. These observations confirm that ICG embedded in a saccharide-based matrix retains its ability to generate reactive oxygen species. The literature indicates that the quantum yield of singlet oxygen production by ICG is lower than that of classical photosensitizers, such as porphyrins or phthalocyanines [6,73], but may be enhanced through structural stabilization of the dye or reduction of its photodegradation [6,75]. In the present work, the results indicate preservation of photochemical activity within a controlled immobilized environment rather than enhancement relative to other systems.

Importantly, in the present study singlet oxygen generation was assessed qualitatively through direct detection of its characteristic near-infrared phosphorescence rather than quantitatively via determination of absolute quantum yield. While this approach provides unequivocal evidence of $^1O_2$ formation, quantitative comparison with reference photosensitizers will require additional measurements under standardized conditions.

The calculated quantum yield is consistent with literature data indicating that indocyanine green exhibits relatively low singlet oxygen generation efficiency in pure aqueous environments, typically around $\Phi_\Delta \approx 0.01$. In contrast, methylene blue shows significantly higher efficiency ($\Phi_\Delta \approx 0.52$), which validates its suitability as a reference standard.

The reduced singlet oxygen generation efficiency of ICG in water can be attributed to several photophysical factors: aggregation of ICG molecules in aqueous media, which reduces intersystem crossing efficiency, increased nonradiative decay pathways, short triplet state lifetime in polar solvents. Additionally, ICG can undergo photooxidative self-degradation upon interaction with generated singlet oxygen, which may further influence observed kinetics. Despite the relatively low quantum yield, the results confirm that ICG remains capable of producing singlet oxygen under the studied conditions. These findings support its use as a photosensitizer, particularly in systems designed to reduce aggregation or enhance photostability, such as immobilized or matrix-based configurations.

In light of these observations, the investigated thin-film saccharide-based system should primarily be regarded as a model platform for studying immobilized ICG under surface-confined

irradiation conditions using indocyanine green. Preservation of absorption and fluorescence properties, as well as the ability to generate singlet oxygen, suggests that such matrices meet key requirements for materials used in localized PDT, where controlled contact of the photosensitizer with tissue and limited diffusion are crucial. The literature reports the effectiveness of surface-based PDT in various clinical areas, such as reduction of bacterial biofilms in the oral cavity using ICG activated by LED light [76], topical photodynamic treatment of skin lesions [77], and laser-assisted PDT for the treatment of onychomycosis [78]. In this context, the present results should be interpreted as demonstrating the photophysical feasibility of immobilized ICG systems rather than as evidence of selective tumor targeting or *in vivo* therapeutic efficacy.

Moreover, owing to their biocompatibility, non-toxicity, and ability to form thin films, high-molecular-weight polysaccharides represent an attractive platform for photomedical applications. Our results indicate that simple saccharide-based surfaces formed from a mixture of sucrose and corn syrup are sufficiently stable to maintain the functional properties of ICG, opening the way for further studies on their use in therapeutic systems and optical imaging methods.

Conclusions

The present study demonstrates that thin-film saccharide-based matrices constitute an effective and reproducible stabilizing environment for indocyanine green. Specifically, the investigated system exhibited a stable absorption maximum at approximately 790 nm and a near-infrared fluorescence maximum around 830 nm, confirming preservation of the characteristic optical response of the dye after immobilization. This work establishes a simplified surface-confined reference model demonstrating that indocyanine green immobilized in thin saccharide-based films retains its fluorescence properties and ability to generate singlet oxygen. Immobilization of the dye within simple saccharide-based films preserved its characteristic absorption and fluorescence properties while preventing aggregation-related spectral degradation. Most importantly, the unequivocal detection of singlet oxygen emission in the 1260–1270 nm range confirms that the photosensitizing activity of ICG is retained after immobilization, highlighting the functional integrity of the ICG–saccharide-based system.

These results provide direct experimental evidence that surface-confined saccharide-based matrices can maintain both the photophysical stability and photochemical functionality of indocyanine green in the solid state. The applied thin-film configuration enables controlled dye immobilization, uniform optical excitation, and efficient oxygen diffusion, which together support reliable assessment of singlet oxygen generation under defined experimental conditions. In contrast to solution-based systems, the applied thin-film configuration enables controlled dye immobilization, uniform optical excitation, and efficient oxygen access, which are critical parameters for reliable assessment of singlet oxygen generation.

From a broader perspective, these findings indicate that thin-film saccharide-based structures represent a useful reference platform for studying photophysical processes relevant to photomedical applications. The combination of biocompatibility, optical accessibility, and preserved photochemical activity makes such systems particularly attractive for surface-based photodynamic approaches, optical sensing, and fluorescence-guided diagnostic strategies. Importantly, the present work addresses the fundamental photophysical feasibility of immobilized ICG systems rather than selective biological targeting or *in vivo* therapeutic performance.

Importantly, the goal of this study was not to demonstrate *in vivo* applicability, but to establish a controlled model system for mechanistic investigation. The results should therefore be interpreted within the limitations of the applied model system. The saccharide-based matrix used in this study represents a simplified, protein-free environment and does not reproduce the complex binding interactions encountered by ICG in biological fluids. Consequently, the relevance of the present results to *in vivo* conditions remains uncertain, and the observations may primarily reflect the behavior of ICG within the artificial model system investigated in this work.

Future studies may include systematic concentration-dependent investigations, optimization of matrix composition, film thickness, hydration level, and irradiation parameters to further enhance photostability and singlet oxygen generation efficiency. Quantitative determination of singlet oxygen quantum yield using established reference photosensitizers under identical experimental conditions will be essential to enable direct comparison with classical PDT agents. Additionally, extending this approach to more complex saccharide-based or hybrid matrices incorporating biologically relevant components, as well as integration of thin-film ICG systems into device-oriented or surface-coated architectures, may facilitate their future application in photomedical materials and localized photodynamic technologies.

References

1. **Zacharioudaki DE**, Fitilis I, Kotti M. Review of fluorescence spectroscopy in environmental quality applications. *Molecules*. 2022;27:4801. doi:10.3390/molecules27154801.
2. **Gu H**, Hu L, Dong Y, Chen Q, Wei Z, Lv R, Zhou Q. Evolving trends in fluorescence spectroscopy techniques for food quality and safety: a review. *J Food Compos Anal*. 2024;131:106212. doi:10.1016/j.jfca.2024.106212.
3. **Dos Santos Rodrigues FH**, Delgado GG, Santana da Costa T, Tasic L. Applications of fluorescence spectroscopy in protein conformational changes and intermolecular contacts. *BBA Adv*. 2023;3:100091. doi:10.1016/j.bbadva.2023.100091.
4. **Chon B**, Ghann W, Uddin J, Anvari B, Kundra V. Indocyanine green fluorescence is dependent on monomer with planar and

twisted structures and inhibited by Haggregation. *Int J Mol Sci*. 2023;24:13030. doi:10.3390/ijms241713030.

5. **Atta D**, Elarif A, Al Bahrawy M. Reactive oxygen species creation by laserirradiated indocyanine green as photodynamic therapy modality: an in vitro study. *Lasers Med Sci*. 2023;38:213. doi:10.1007/s10103-023-03876-1.
6. **Mytych W**, CzarneckaCzapczyńska M, BartusikAebisher D, Aebisher D, Henrykowska G, KawczykKrupka A. Evaluation of selective efficacy of indocyanine greenmediated photodynamic therapy in MCF7 breast cancer cells compared to healthy cells in a 3D hollow fiber bioreactor model. *Pharmaceuticals*. 2025;18:1832. doi:10.3390/ph18121832.
7. **Tseng HC**, Kuo CY, Liao WT, Chou TS, Hsiao JK. Indocyanine green as a nearinfrared theranostic agent for ferroptosis and apoptosisbased, photothermal, and photodynamic cancer therapy. *Front Mol Biosci*. 2022;9:1045885. doi:10.3389/fmolb.2022.1045885.
8. **Gowsalya K**, Yasothamani V, Vivek R. Emerging indocyanine greenintegrated nanocarriers for multimodal cancer therapy: a review. *Nanoscale Adv*. 2021;3:33323352. doi:10.1039/d1na00059d.
9. **Reinhart MB**, Huntington CR, Blair LJ, Heniford BT, Augenstein VA. Indocyanine green: historical context, current applications, and future considerations. *Surg Innov*. 2016;23:166175. doi:10.1177/1553350615604053.
10. **Wang H**, Li X, Tse BW, Yang H, Thorling CA, Liu Y, et al. Indocyanine greenincorporating nanoparticles for cancer theranostics. *Theranostics*. 2018;8:12271242. doi:10.7150/thno.22872.
11. **Zhang X**, Li Y, Zhou Y, Mao F, Lin Y, Guan J, Sun Q. Diagnostic performance of indocyanine greenguided sentinel lymph node biopsy in breast cancer: a metaanalysis. *PLoS One*. 2016;11:e0155597. doi:10.1371/journal.pone.0155597.
12. **Lim C**, Vibert E, Azoulay D, Salloum C, Ishizawa T, Yoshioka R, et al. Indocyanine green fluorescence imaging in the surgical management of liver cancers: current facts and future implications. *J Visc Surg*. 2014;151:117124. doi:10.1016/j.jviscsurg.2013.11.003.
13. **Mihara M**, Hara H, Araki J, Kikuchi K, Narushima M, Yamamoto T, et al. Indocyanine green lymphography is superior to lymphoscintigraphy for diagnostic imaging of early lymphedema of the upper limbs. *PLoS One*. 2012;7:e38182. doi:10.1371/journal.pone.0038182.
14. **Chakedis JM**, Maser C, Brumund KT, Bouvet M. Indocyanine green fluorescenceguided redo parathyroidectomy. *BMJ Case Rep*. 2015;2015:bcr2015211778. doi:10.1136/bcr-2015-211778.
15. **Duprée A**, Rieß H, Detter C, Debus ES, Wipper SH. Utilization of indocyanine green fluorescent imaging for assessment of microperfusion in vascular medicine. *Innov Surg Sci*. 2018;3:193201. doi:10.1515/iss-2018-0014.
16. **Ara ES**, Noghreiyan AV, Sazgarnia A. Evaluation of photodynamic effect of indocyanine green on colon and glioblastoma cancer cell lines pretreated by cold atmospheric plasma. *Photodiagn Photodyn Ther*. 2021;35:102408. doi:10.1016/j.pdpdt.2021.102408.
17. **Liu G**, Zhang T. Singlecopy oligonucleotide fluorescence in situ hybridization probe design platforms: development, application and evaluation. *Int J Mol Sci*. 2021;22:7124. doi:10.3390/ijms22137124.
18. **Seo SH**, Bae MG, Park HJ, Ahn JS, Lee JW. Study of optimal conditions affecting the photothermal effect and fluorescence characteristics of indocyanine green. *Curr Opt Photonics*. 2021;5:554561.
19. **Choromańska A**, Kulbacka J, Saczko J. Terapia fotodynamiczna – założenia, mechanizm, aplikacje kliniczne. *Nowa Medycyna*. 2013;1:2630.
20. **Krajewska E**, Bryszewska M. Terapia fotodynamiczna. Łódź: *Wydawnictwo Uniwersytetu Łódzkiego*; 1999.
21. **Kwaśny M**. Metoda fotodynamicznego leczenia w dermatologii. *Forum Dermatologiczne*. 2018;4:138–147.
22. **Dolmans DE**, Fukumura D, Jain RK. Photodynamic therapy for cancer. *Nat Rev Cancer*. 2003;3:380387. doi:10.1038/nrc1071.
23. **Lange N**, Szlasa W, Saczko J, Chwiłkowska A. Potential of cyaninederived dyes in photodynamic therapy. *Pharmaceutics*. 2021;13:818. doi:10.3390/pharmaceutics13060818.
24. **Vallejo MCS**, Moura NMM, Gomes ATPC, Joaquinito ASM, Faustino MAF, Almeida A, et al. The role of porphyrinoid photosensitizers for skin wound healing. *Int J Mol Sci*. 2021;22:4121. doi:10.3390/ijms22084121.
25. **Aebisher D**, Serafin I, BatógSzczęch K, Dynarowicz K, Chodurek E, KawczykKrupka A, BartusikAebisher D. Photodynamic therapy in the treatment of cancer: the selection of synthetic photosensitizers. *Pharmaceuticals*. 2024;17:932. doi:10.3390/ph17070932.
26. **Chen J**, Zhu Y, Kaskel S. Porphyrinbased metalorganic frameworks for biomedical applications. *Angew Chem Int Ed Engl*. 2021;60:50105035. doi:10.1002/anie.201909880.
27. **Mahmut Z**, Zhang C, Ruan F, Shi N, Zhang X, Wang Y, et al. Medical applications and advancement of nearinfrared photosensitive indocyanine green molecules. *Molecules*. 2023;28:6085. doi:10.3390/molecules28166085.
28. **Han YH**, Kankala RK, Wang SB, Chen AZ. Leveraging engineering of indocyanine greenencapsulated polymeric nanocomposites for biomedical applications. *Nanomaterials*. 2018;8(6):360. doi:10.3390/nano8060360.
29. **Dash BS**, Das S, Chen JP. Photosensitizerfunctionalized nanocomposites for lightactivated cancer theranostics. *Int J Mol Sci*. 2021;22:6658. doi:10.3390/ijms22136658.
30. **Monzavi A**, Chinipardaz Z, Mousavi M, Fekrazad R, Moslemi N, Azaripour A, et al. Antimicrobial photodynamic therapy using diode laseractivated indocyanine green as an adjunct in chronic periodontitis. *Photodiagn Photodyn Ther*. 2016;14:9397. doi:10.1016/j.pdpdt.2016.02.007.

31. **Sheng Z**, Hu D, Xue M, He M, Gong P, Cai L. Indocyanine green nanoparticles for theranostic applications. *NanoMicro Lett*. 2013;5:145150.
32. **Costa RA**, Farah ME, Cardillo JA, Belfort R Jr. Photodynamic therapy with indocyanine green for occult subfoveal choroidal neovascularization in AMD. *Curr Eye Res*. 2001;23:271275. doi:10.1076/ceyr.23.4.271.5449.
33. **Lee YH**, Chung CL. Thermoresponsive composite hydrogel loaded with indocyanine green and camptothecin for postsurgical skin cancer photochemotherapy. *Gels*. 2025;11:71. doi:10.3390/gels11010071.
34. **Lee SS**, Choi Y. Nearinfrared dyeloaded thermosensitive hydrogels as novel fluorescence tissue markers. *Gels*. 2025;11:649. doi:10.3390/gels11080649.
35. **Gutberlet B**, Preis E, Roschenko V, Bakowsky U. Photothermally controlled drug release of PLA nanofibers loaded with indocyanine green and curcumin for antimicrobial PDT. *Pharmaceutics*. 2023;15:327. doi:10.3390/pharmaceutics15020327.
36. **Siddiqua A**, Clutter E, Garklavs O, Kanniyappan H, Wang RR. Electrospun silkICG composite fibers for hemorrhage control. *J Funct Biomater*. 2024;15:272. doi:10.3390/jfb15090272.
37. **Chen X**, Zou J, Zhang K, Zhu J, Zhang Y, Zhu Z, et al. Photothermal/MMP2 dualresponsive gelatin nanoparticles for breast cancer treatment. *Acta Pharm Sin B*. 2021;11:271282. doi:10.1016/j.apsb.2020.08.009.
38. **Yang C**, Lei J, Kang X, Zhang P, Zheng S, Li Q, et al. Yeast cell wallderived hybrid hydrogel with photothermal and immune combined therapy for melanoma. *Int J Nanomedicine*. 2023;18:54235440. doi:10.2147/IJN.S409674.
39. **Murphy EJ**, Fehrenbach GW, Abidin IZ, Buckley C, Montgomery T, Pogue R, et al. Polysaccharides as naturally occurring immune modulators. *Polymers*. 2023;15:2373. doi:10.3390/polym15102373.
40. **Benalaya I**, Alves G, Lopes J, Silva LR. Natural polysaccharides: sources, characteristics, properties, food and pharmaceutical applications. *Int J Mol Sci*. 2024;25:1322. doi:10.3390/ijms25021322.
41. **Damiri F**, Fatimi A, Liu Y, Musuc AM, Fajardo AR, Gowda BHJ, et al. Recent advances in 3D bioprinted polysaccharide hydrogels for biomedical applications: a comprehensive review. *Carbohydr Polym*. 2025;348:122845. doi:10.1016/j.carbpol.2024.122845.
42. **Dattilo M**, Patitucci F, Prete S, Parisi OI, Puoci F. Polysaccharidebased hydrogels and their application as drug delivery systems in cancer treatment: a review. *J Funct Biomater*. 2023;14:55. doi:10.3390/jfb14020055.
43. **Burloiu AM**, Ozon EA, Musuc AM, Anastasescu M, Socoteanu RP, Atkinson I, et al. Porphyrin photosensitizers into polysaccharidebased biopolymer hydrogels for topical photodynamic therapy: physicochemical and pharmacotechnical assessments. *Gels*. 2024;10:499. doi:10.3390/gels10080499.
44. **Haidekker MA**, Brady TP, Lichlyter D, Theodorakis EA. Effects of solvent polarity and viscosity on fluorescent properties of molecular rotors and related probes. *Bioorg Chem*. 2005;33:415425. doi:10.1016/j.bioorg.2005.07.005.
45. **Szewczyk G**, Mokrzyński K. Concentrationdependent photoproduction of singlet oxygen by common photosensitizers. *Molecules*. 2025;30:1130. doi:10.3390/molecules30051130.
46. **Kurczewska J**. Recent reports on polysaccharidebased materials for drug delivery. *Polymers*. 2022;14:4189. doi:10.3390/polym14194189.
47. **Liu S**, Tang J, Ji F, Lin W, Chen S. Recent advances in zwitterionic hydrogels: preparation, properties and biomedical applications. *Gels*. 2022;8:46. doi:10.3390/gels8010046.
48. **Ozon EA**, Anastasescu M, Musuc AM, Burloiu AM, Socoteanu RP, Atkinson I, et al. Formulation and characterization of Carbopolbased porphyrin gels for targeted dermatooncological therapy. *Int J Mol Sci*. 2025;26:3641. doi:10.3390/ijms26083641.
49. **Lee JH**, Kim KH, Kwon OH, Kwon OK, Uyama H, Kim YJ. Photodynamic activity of protoporphyrin IXimmobilized cellulose monolith for nerve tissue regeneration. *Int J Mol Sci*. 2022;23:1035. doi:10.3390/ijms23031035.
50. **SmolarkiewiczWyczachowski A**, Kaczmarek H, Piskorz J, Nowak P, ZieglerBorowska M. Chitosan composites containing borondipyrromethene derivatives for biomedical applications. *Int J Mol Sci*. 2023;24:1770. doi:10.3390/ijms24021770.
51. **Lin J**, Jiao G, KermanshahiPour A. Algal polysaccharidebased hydrogels: extraction, synthesis, characterization and applications. *Mar Drugs*. 2022;20(5):306. doi:10.3390/md20050306.
52. **Evident Scientific**. BX51 fluorescence lightpaths tutorial. Available from: https://evidentscientific.com/en/microscope-resource/tutorials/lightpaths/bx51fluorescence (evidentscientific.com in Bing).
53. **Saboural P**, Chaubet F, Rouzet F, AlShoukr F, Azzouna RB, Bouchemal N, et al. Purification of lowmolecularweight fucoidan for SPECT molecular imaging of myocardial infarction. *Mar Drugs*. 2014;12:48514867. doi:10.3390/md12094851.
54. **Agilent Technologies**. Cary 60 UVVis brochure. Available from: https://www.agilent.com/cs/library/brochures/5990-7789EN_Cary_60_UV-Vis_Brochure.pdf (agilent.com in Bing).
55. **Agilent Technologies**. Cary Eclipse fluorescence spectrophotometer brochure. Available from: https://www.agilent.com/cs/library/brochures/5990-7788EN_Cary_Eclipse_Brochure.pdf (agilent.com in Bing).
56. **Agilent Technologies**. Cary Eclipse fluorescence spectrophotometer system page. Available from: https://www.agilent.com/en/product/molecular-spectroscopy/fluorescence-spectroscopy/fluorescence-systems/cary-eclipse-fluorescence-spectrophotometer (agilent.com in Bing).
57. **PicoQuant**. FluoTime 300 datasheet. Available from: https://www.picoquant.com/images/uploads/downloads/datasheet_fluotime300.pdf (picoquant.com in Bing).
58. **Kawaska**. FluoTime 300 product page. Available from: https://kawaska.pl/produkt/fluotime-300/ (kawaska.pl in Bing).
59. **Starosolski Z**, Bhavane R, Ghaghada KB, Vasudevan SA, Kaay A, Annapragada A. Indocyanine green fluorescence in the second

nearinfrared (NIRII) window. *PLoS One*. 2017;12:e0187563. doi:10.1371/journal.pone.0187563.

60. **Shao C**, Xiao F, Guo H, Yu J, Jin D, Wu C, et al. Polymer micelles controlling dye Jaggregation to enhance theranostic capability. *iScience*. 2019;22:229239. doi:10.1016/j.isci.2019.11.022.
61. **Yaseen MA**, Yu J, Wong MS, Anvari B. Stability assessment of indocyanine green within dextrancoated mesocapsules by absorbance spectroscopy. *J Biomed Opt*. 2007;12:064031. doi:10.1117/1.2821423.
62. **Rodriguez VB**, Henry SM, Hoffman AS, Stayton PS, Li X, Pun SH. Encapsulation and stabilization of indocyanine green within poly(styrenealtmaleic anhydride) blockpoly(styrene) micelles for nearinfrared imaging. *J Biomed Opt*. 2008;13:014025. doi:10.1117/1.2834296.
63. **Chiba R**, Ebihara Y, Shiiya H, Ujiie H, FujiwaraKuroda A, Kaga K, et al. A novel system for analyzing indocyanine green fluorescence spectra enables deeper lung tumor localization during thoracoscopic surgery. *J Thorac Dis*. 2022;14:29432952. doi:10.21037/jtd-22-244.
64. **Novo DC**, Edgar KJ. Smart fluorescent polysaccharides: recent developments and applications. *Carbohydr Polym*. 2024;324:121471. doi:10.1016/j.carbpol.2023.121471.
65. **Ciaramitaro V**, Szpunar M, Vitale F, Tornatore E, Presentato A, Alduina R, et al. Chitosan, alginate and carboxymethyl cellulosebased film for controlled release of indocyanine green for antibiofilm applications. *Carbohydr Polym Technol Appl*. 2025;10:100828. doi:10.1016/j.carpta.2025.100828.
66. **Swierczewska M**, Han HS, Kim K, Park JH, Lee S. Polysaccharidebased nanoparticles for theranostic nanomedicine. *Adv Drug Deliv Rev*. 2016;99:7084. doi:10.1016/j.addr.2015.11.015.
67. **Markuszewski M**, BuszewskaForajta M, Artymowicz M, Połom W, Roslan M, Markuszewski M. Binding of indocyanine green to human serum albumin potentially improves sentinel lymph node detection. *Arch Med Sci*. 2021;18:719725. doi:10.5114/aoms/113237.
68. **Jang HJ**, Song MG, Park CR, Youn H, Lee YS, Cheon GJ, Kang KW. Imaging of indocyanine green–human serum albumin complex in SPARCexpressing glioblastoma. *Int J Mol Sci*. 2023;24:850. doi:10.3390/ijms24010850.
69. **Uthaman S**, Lee SJ, Cherukula K, Cho CS, Park IK. Polysaccharidecoated magnetic nanoparticles for imaging and gene therapy. *Biomed Res Int*. 2015;2015:959175. doi:10.1155/2015/959175.
70. **Deshpande N**, Ramesh A, Nandi D, Nguyen A, Brouillard A, Kulkarni A. Supramolecular polysaccharide nanotheranostics that inhibit cancer cell growth and monitor targeted therapy response. *Nanotheranostics*. 2020;4:156172. doi:10.7150/ntno.44703.
71. **Zayed A**, ElAasr M, Ibrahim AS, Ulber R. Fucoidan characterization: determination of purity and physicochemical and chemical properties. *Mar Drugs*. 2020;18(11):571. doi:10.3390/md18110571.
72. **Herdiana Y**, Wathoni N, Shamsuddin S, Joni IM, Muchtaridi M. Chitosanbased nanoparticles for targeted drug delivery in breast cancer treatment. *Polymers*. 2021;13:1717. doi:10.3390/polym13111717.
73. **Herdiana Y**, Wathoni N, Gozali D, Shamsuddin S, Muchtaridi M. Chitosanbased nanosmart drug delivery system in breast cancer therapy. *Pharmaceutics*. 2023;15:879. doi:10.3390/pharmaceutics15030879.
74. **Yu TC**, Davis SJ, Scimone MT, Grimble J, Maguluri G, Anand S, et al. Highsensitivity singlet oxygen luminescence sensor using computational spectroscopy and solidstate detector. *Diagnostics*. 2023;13:3431. doi:10.3390/diagnostics13223431.
75. **Pola M**, Kolarova H, Bajgar R. Generation of singlet oxygen by porphyrin and phthalocyanine derivatives regarding oxygen level. *J Med Sci*. 2022;91:e752. doi:10.20883/medical.e752.
76. **Nikinmaa S**, Moilanen N, Sorsa T, Rantala J, Alapulli H, Kotiranta A, et al. Indocyanine greenassisted and LEDlightactivated antibacterial photodynamic therapy reduces dental plaque. *Dent J*. 2021;9:52. doi:10.3390/dj9050052.
77. **Zhang W**, Jin Z, Gao T, Fan L, Wang W, Zeng X, Qin L. Topical 5aminolevulinic acid photodynamic therapy for recalcitrant facial flat warts. *Photodiagn Photodyn Ther*. 2024;45:103934. doi:10.1016/j.pdpdt.2023.103934.
78. **Abdallah M**, AbuGhali MM, ElSayed MT, Soltan MY. Fractional CO_2assisted photodynamic therapy improves clinical outcome and patient satisfaction in toenail onychomycosis: intrapatient comparative study. *J Dermatolog Treat*. 2022;33:542549. doi:10.1080/09546634.2020.1771252.